Experimental Parasitology 143 (2014) 74–82

Contents lists available at ScienceDirect

Experimental Parasitology

journal homepage: www.elsevier.com/locate/yexpr

Morphological and molecular studies of *Vairimorpha necatrix* BM, a new strain of the microsporidium *V. necatrix* (microsporidia, burenellidae) recorded in the silkworm, *Bombyx mori*

Bo Luo [a], Handeng Liu [b], Guoqing Pan [a,*], Tian Li [a], Zeng Li [a], Xiaoqun Dang [c], Tie Liu [a], Zeyang Zhou [a,c]

[a] State Key Laboratory of Silkworm Genome Biology, Southwest University, Chongqing 400716, PR China
[b] Experimental Teaching Center, Chongqing Medical University, Chongqing 400016, PR China
[c] Laboratory of Animal Biology, Chongqing Normal University, Chongqing 400047, PR China

HIGHLIGHTS

- This is a new study on the *Vairimorpha necatrix* recorder in the silkworm *Bombyx mori*.
- Diplokaryotic spores ($4.7 \pm 0.2 \times 2.1 \pm 0.2$ μm) had isofilar polar filaments with 13–17 coils.
- Almost all the tissues of silkworm were the targets for *Vairimorpha necatrix* BM but no infection in the ovary.
- There is no vertical transmission in silkworm after *Vairimorpha necatrix* BM infection.

GRAPHICAL ABSTRACT

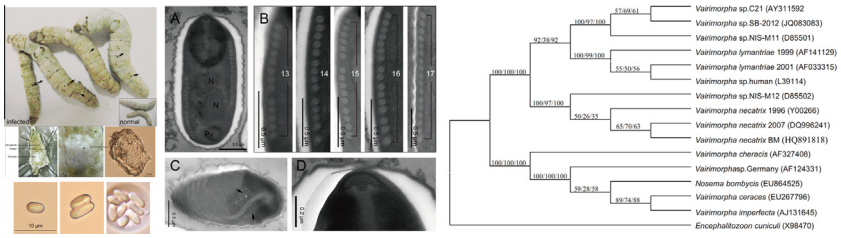

ARTICLE INFO

Article history:
Received 28 December 2013
Received in revised form 21 April 2014
Accepted 1 May 2014
Available online 10 May 2014

Keywords:
Silkworm
Microsporidia
V. necatrix
Ultrastructure
Vertical transmission

ABSTRACT

Vairimorpha sp. BM (2012) is a recent isolate of the microsporidia from the silkworm in Shandong, China. The ultrastructure, tissue pathology and molecular characterization of this isolate is described in this study. This pathogenic fungus causes pebrine disease in silkworms which manifests as a systemic infection. Meanwhile, the silkworm eggs produced by the infected moths were examined using a microscope and PCR amplification. Neither spores nor the expected PCR band were observed, suggesting that no vertical transmission occurred in *Bombyx mori*. In addition, the ultrastructure of the isolate was studied by light microscopy and transmission electron microscopy. Two types of spores were observed: diplokaroytic spores with 13–17 coils of polar tubes and monokaryotic spores with less coils of polar tubes which could form octospores; however, no sporophorous vesicles were observed. Finally, phylogenetic analysis of the small subunit rRNA genes of *Vairimorpha* species showed that this isolate has a closer relationship to *Vairimorpha necatrix* than the other species studied. This result also is supported by phylogenetic analysis based on their actin genes, heat shock protein 70 (*HSP70*) and RNA polymerase II (*RPB1*). Based on the information gained during this study, we propose that this microsporidian species infecting *B. mori* should be given the name *V. necatrix* BM.

Published by Elsevier Inc.

1. Introduction

The silkworm, *Bombyx mori* (Lepidoptera: Bombycidae), which has been used to produce silk for 5000 years, is one of the most economically important insects. This species plays an important

* Corresponding author. Fax: +86 23 68251128.
E-mail address: gqpan@swu.edu.cn (G. Pan).

http://dx.doi.org/10.1016/j.exppara.2014.05.001
0014-4894/Published by Elsevier Inc.

role financially for farmers in many countries, including, China, India and Thailand (Xia et al., 2004; Goldsmith et al., 2005; Prasad et al., 2005), but it is vulnerable to disease during growth. Pebrine disease is caused by the microsporidian *Nosema bombycis* (Nageli 1857). This disease is a big threat to the sericulture industry due to heavy financial loss caused by vertical transmission (Bhat et al., 2009). The pathogenicity and ultrastructure of *N. bombycis* has been studied extensively since the microorganism was first identified (Ishihara et al., 1966; Ishihara, 1969; Sato et al., 1982). *N. bombycis* is the most typical microsporidian species that causes silkworm pebrine disease, but it is not the only cause of the disease; other *Nosema* and *Vairimorpha* species have been found in the infected silkworms (Hatakeyama et al., 1997; Nageswara et al., 2004; Wang et al., 2006).

The microsporidian *Vairimorpha* sp. BM was first isolated from infected domesticated silkworms in Shandong, China. It was grouped with *Vairimorpha* based on rRNA. Since it has more than 13 polar tube coils, a posterior vacuole, and is dikaryotic, it was named *Vairimorpha* sp. BM (Liu et al., 2012). Six chromosome bands were separated by pulsed field gel electrophoresis. The sequences of SSU rRNA shared homology with members of the *Vairimorpha* genus. However, whether this isolate is a new species or a known species is still unknown.

The genus *Vairimorpha* was established from a microsporidian species isolated from *Trichoplusia ni* (Pilley, 1976) using the specific name *Vairimorpha necatrix* (Kramer, 1965). This is a promising species for microbial control due to its virulence and prolificity in lepidopterous pests, and is the most prevalent parasite of insects in the field (Mitchell and Cali, 1993; Down et al., 2004). Although China is the major producer of silk in the world, there are few reports concerning the symptoms, infective circulation, pathology, prevention and treatment of *Vairimorpha* species isolated from silkworms in China. To determine whether the microsporidian *Vairimorpha* sp. BM is a new or a reported species, we studied the tissue pathology, ultrastructure and characterized at the molecular level. The results showed that the parasite isolated from silkworm is similar to *V. necatrix*. In result, we classify this isolate as a new strain of *V. necatrix* and propose to rename it *V. necatrix* BM (*B. mori*).

2. Materials and methods

2.1. Insects and microsporidia

Egg masses of the silkworm *B. mori* (Dazao) were obtained from the State Key Laboratory of Silkworm Genome Biology at Southwest University of China. Silkworm larvae were reared with fresh mulberry leaves at 25 °C. The microsporidian *V. necatrix* BM identified by Liu et al. (2012) was isolated from infected silkworms in Shandong, China. The fresh *V. necatrix* BM spores used in these experiments were produced in silkworms. The third instar, molted silkworm larvae were challenged by feeding on fresh mulberry leaves contaminated with *V. necatrix* BM (approximately 10^5 spores per silkworm) (Liu et al., 2008). The infected larvae were then dissected on the 5th day of the fifth instar. The midgut tissues, silk glands, malpighian tubules, fat bodies and gonads were extracted and fixed in 2.5% (v/v) glutaraldehyde and stored at 4 °C for light microscopy (LM) and transmission electron microscopy (TEM).

2.2. Pebrine inspection of silkworm eggs

The simulation model of microsporidian infection was completed by inoculating 10^4 spores for every newly exuviated silkworm in the 5th instar. Afterwards, silkworms were maintained normally to obtain silkworm eggs. Then, DNA was extracted from the resulting silkworm eggs using the KOH method (Hatakeyama and Hayasaka, 2003). PCR primers were designed using specific sequences that discriminated between the silkworm and *V. necatrix* BM, as reported previously (Huang et al., 2004). Control primers specific for actin3 were designed using silkworm genomic sequences (Table 1). The amplification was performed under the following conditions: after initial denaturation of DNA at 94 °C for 5 min, 30 cycles were run at 94 °C for 1 min, followed by annealing at 58 °C for 1 min, and extension at 72 °C for 2 min, with a final extension at 72 °C for 10 min. PCR products were analysed by electrophoresis on 1.0% agarose gels and visualized by ethidium bromide staining.

Table 1
Primers used for pebrine detection of silkworm eggs.

Primers	Target species	Sequence
18f	*V. necatrix* BM	5′-CACCAGGTTGATTCTGCC-3′
1537r		5′-TTATGATCCTGCTAATGGTTC-3′
Actin3-F	*B. mori*	5′-AACACCCCGTCCTGCTCACTG-3′
Actin3-R		5′-GGGCGAGACGTGTGATTTCCT-3′

2.3. Light microscopy and transmission electron microscopy

Smears of the infected tissues and live spores were studied using a light microscope (Olympus BX51 TRF). Digital pictures were acquired with the Microscope USB Camera (Olympus DP71). Electron microscopy was performed as previously described (Liu et al., 2012), with slight modifications. Segments from infected larvae were fixed in a 2.5% (v/v) glutaraldehyde solution buffered in 0.1 M Na cacodylate (pH 7.4) for 2.5 h at 4 °C, post-fixed in aqueous 1% (w/v) OsO_4 (pH 7.4) for 3 h at room temperature, dehydrated using a graded ethanol series and embedded in Epon-Araldite. Ultrathin sections (60–100 nm) were stained with 2% (w/v) uranyl acetate in 50% ethanol followed by Reynolds' lead citrate and examined using a TECNA100-Philips electron microscope at an accelerating voltage of 80 kV.

2.4. Molecular characterization

All the small subunit rRNA (SSU rRNA) sequences were obtained from the GenBank database in the National Center for Biotechnology Information (NCBI) and were aligned using the ClustalX 1.83 program. The rRNA gene sequence of *Encephalitozoon cuniculi* was used as an out-group. The partial sequences of actin gene, heat shock protein 70 (*HSP70*) and RNA polymerase II (*RPB1*) of *V. necatrix* BM were retrieved from the genomic data. The genomic sequence reads were obtained by Solexa sequencing. To assemble the *V. necatrix* BM genome, the Solexa reads were assembled by BGI's de novo assembly software (Li et al., 2010). The genes actin, *HSP70* and *RPB1* of *V. necatrix* were downloaded from the NCBI GenBank database and were aligned with *V. necatrix* BM using the ClustalX 1.83 program. In addition, the neighbor-joining (NJ), maximum parsimony (MP) and minimum evolution (ME) trees (Saitou and Nei, 1987; Saitou and Imanishi, 1989) were reconstructed using the MEGA 4.0 program (Tamura et al., 2007). Bootstrap values were evaluated based on 1000 replicates for NJ tree and 100 replicates for ME and MP trees.

3. Results

3.1. Pathogenic characteristics

In the late stages of infection, the infected larvae showed obvious symptoms of disease. First, the body color changed from white

to yellow, and the body length was reduced. Secondly, the infected larvae exhibited symptoms such as diarrhea and the appearance of brown spots on the posterior surface of the body (Fig. 1). Moreover, the entire midgut of the infected larva became swollen, yellow–brown in color, and white cysts developed. Localized infection developed as tumor-like masses around the midgut which were full of spores. The malpighian tubules and silk glands, however, looked normal (Fig. 2). Finally, light microscopy revealed that a large number of spores were present in the midgut, fat body and spermary compared to the silk gland and malpighian tubules in which there were rarely a few spores. Notably, no spores were observed in the ovary, suggesting that this microsporidia might not be transmitted vertically (Fig. S1).

3.2. Vertical transmission investigation

To survey whether *V. necatrix* BM could be vertically transmitted in the silkworm, the spores in silkworm eggs and larvae produced by *V. necatrix* BM infected moths were evaluated using light microscopy and PCR. Over 100 eggs and 100 hatched larvae per stage 1–3 were studied. No spores were observed in eggs and all of the larval stages, and the larvae were all healthy with no fatalities. However, in the control group, eggs from moths infected with *N. bombycis* were evaluated, and twenty-five eggs were found to be infected (Table S1). Furthermore, PCR detection of silkworm-egg infection showed the same results observed with light microscopy. Two PCR primers (SSU for *V. necatrix* BM and Actin3 for silkworm) were used for pebrine inspection of silkworm eggs, but no signal was detected for SSU in the PCR products derived from silkworm eggs using these two primer pairs (Fig. 3). This experiment was repeated twice, and the same results were obtained both times, suggesting that *V. necatrix* BM does not transmit from the female moth to her eggs.

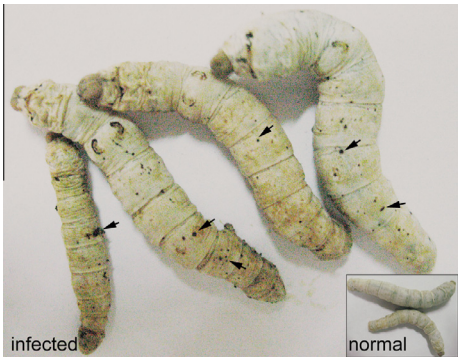

Fig. 1. Silkworm larvae with *V. necatrix* BM infection compared with the healthy individuals (bottom right). The infected larvae shows obvious symptoms of disease compared with the healthy larvae. The body color changed from white to yellow, symptoms such as diarrhea were exhibited, and brown spots appeared on the posterior surface of the body (arrows). (For interpretation of the references to color in this figure legend, the reader is referred to the web version of this article.)

3.3. Light and electron microscopy observations

V. necatrix BM is polymorphic in its life cycle. The mature spores were oval-to kidney-shaped with an average size of $4.7 \pm 0.2 \times 2.1 \pm 0.2$ μm. They are similar to those of *Vairimorpha plodiae* (with an average size of 4.7×2.5) and *V. necatrix*, based on isolates from China in 1992 (with an average size of $4.88 \pm 0.27 \times 2.47 \pm 0.11$) and from *Pseudaletia unipuncta* in 2004 (with an average size of $4.82 \pm 0.07 \times 2.01 \pm 0.02$). The size is obviously different from *N. bombycis* (with an average size of $3.82 \pm 0.2 \times 2.34 \pm 0.15$). Octospores were observed to be refractive under phase contrast microscopy, but no sporophorous vesicles were observed. All octospores were monokaryotic at all stages and were only observed in the moths (Fig. 4 and Table 2).

In our previous study (Liu et al., 2012), the rough ultrastructure of mature spores isolated from silkworms indicated that there were no remarkable differences in their primary structure compared with other *Vairimorpha* species. In this study, transmission electron microscopy (TEM) of midgut and fat body tissues infected by *V. necatrix* BM were performed. These micrographs showed a more detailed level of ultrastructure in *V. necatrix* BM.

Merogony occurred once the sporoplasm entered the host cell. The proliferative cells, referred to as meronts, were roundish cells observed in the fat body in the early stage of the diplokaryotic secondary sporulation cycle (S2ss). They had a large nuclear region with either a single or double nuclei (diplokaryon). No dominant endoplasmic reticulum (ER) or Golgi vesicles were observed in the cytoplasm. Host mitochondria were observed surrounding microsporidia in the early merogonial stage (Fig. 5A–C). The meront then divided into two diplokaryotic meronts by binary fission. The endoplasmic reticulum was visible at this stage (Fig. 5D). The developmental meront then divided with three or four nuclei in a sporophorous vesicle (Fig. 5E and F), which was the pre-sporogony stage for diplokaryotic spores and octospores.

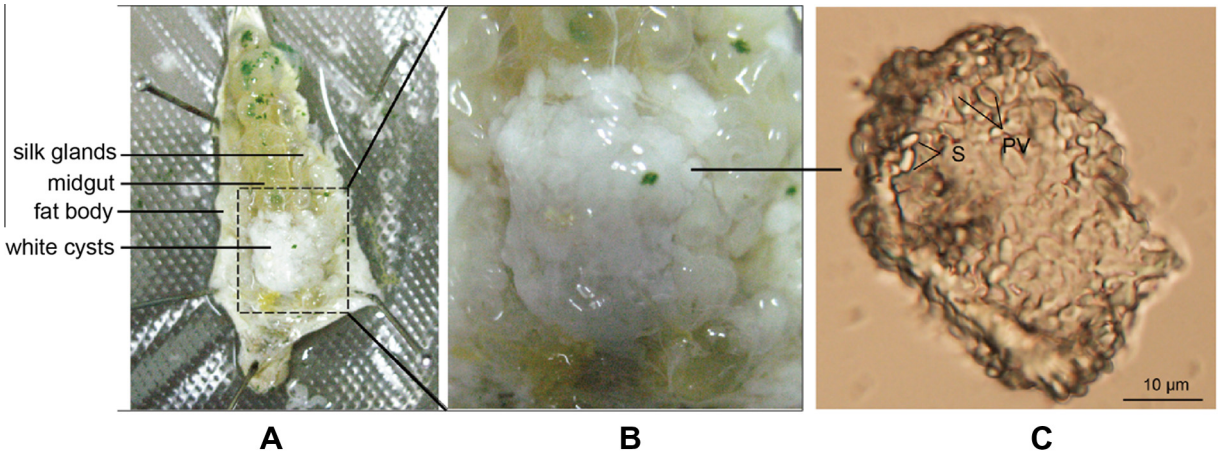

Fig. 2. Photographs of *B. mori* infected with the microsporidian parasite *V. necatrix* BM. (A) The infected silkworm larva was dissected at the 5th day of the fifth instar. White cysts which developed as tumor-like masses around the midgut were visible. (B) An enlarged image of the dotted box in figure A; the white cysts were full of spores. (C) Ellipsoidal spores (*S*) with their polar vacuoles (*PV*) were observed.

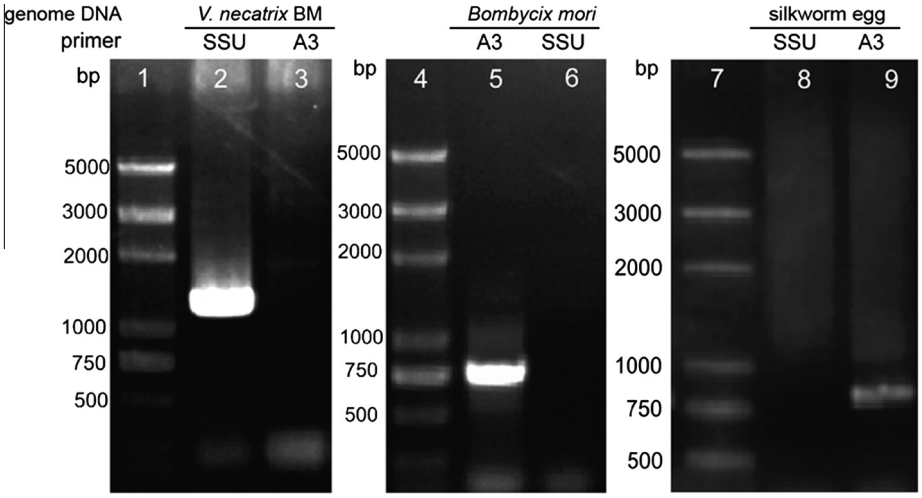

Fig. 3. Evaluation of pebrine disease in silkworm eggs using PCR. SSU primers were specific for *V. necatrix* BM, and Actin3 primers were specific for silkworm. Three different genomic DNAs were prepared from *V. necatrix* BM, silkworms, and silkworm eggs. Lanes 1; 4; 7: Trans 2000 DNA marker; Lanes 2–3: PCR products of genomic DNA from *V. necatrix* BM; the PCR analysis indicated that the SSU primers were specific. Lanes 5–6: PCR products from silkworm genomic DNA; the PCR analysis showed that the Actin3 primers were specific. Lanes 8–9: PCR products from the genomic DNA from silkworm eggs; no signal was detected for SSU in the PCR products derived from silkworm eggs (lane 8), which indicated that there were no spores in silkworm eggs. The PCR products in lane 9 used as positive control.

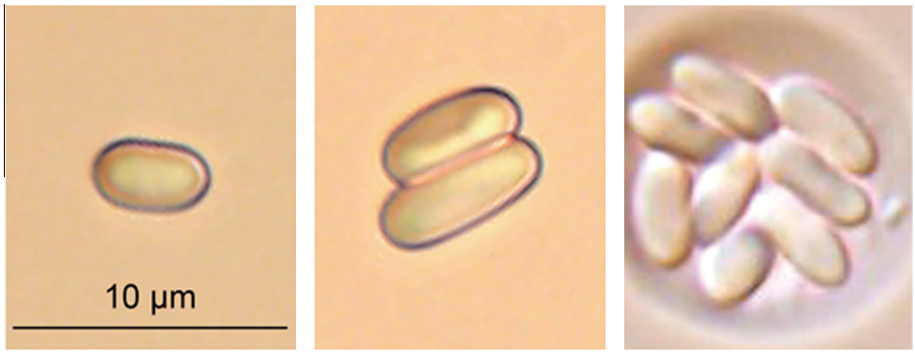

Fig. 4. Micrographs of *V. necatrix* BM spores in the silkworm. (A) Micrographs of an unfixed, monokaryotic spore from the silkworm larvae. (B) Micrographs of two unfixed, diplokaryotic spores from the silkworm larvae. (C) Octospores in tissues of infected moths, the octospores were observed to be refractive under phase contrast microscopy, no sporophorous vesicle was observed. All scale bars, 10 μm.

Table 2
Morphometric data for diplokaryotic spores of microsporidia isolated from *B. mori* and other *Vairimorpha* species.

Microsporidian species	Host species	Fresh spores (μm)		Polar filament coins
		Length	Width	
Vairimorpha necatrix (China)	*Hwliothis armigera*	4.88 ± 0.27	2.47 ± 0.11	14–16
Vairimorpha necatrix	*Pseudaletia unipuncta*	4.82 ± 0.07	2.01 ± 0.02	14–20
Vairimorpha necatrix	*H. zea*	4.4	2.3	12–14
Vairimorpha ephestiae	*Ephestia elutella*	4.0–4.5	2.0–2.5	16
Vairimorpha heterosporum	*H. zea*	4.2	2.4	10–18
Vairimorpha plodiae	*H. zea*	4.7	2.5	13–16
Vairimorpha imperfecta	*Plutella xylostella*	4.3 ± 0.1	2.0 ± 0.1	15.5
Vairimorpha mesnili	*Pieris rapae*	3.84 ± 0.03	1.82 ± 0.01	10–13
Vairimorpha disparis	*Lymantria dispar*	5.4 ± 0.48	2.5 ± 0.37	11–13
Nosema bombycis	*Bombyx mori*	3.82 ± 0.2	2.34 ± 0.15	13–14
Vairimorpha necatrix BM	*Bombyx mori*	4.7 ± 0.2	2.1 ± 0.2	13–17

The sporogony phase involves the development of a meront into a sporont, the cell that produces the sporoblasts. Sporoblasts are cells that mature and transform into spores without further division (Wang et al., 2009). Spores at the stage of sporogony were abundant in the midgut, where there were primarily sporonts and sporoblasts. The early sporogony phase involved thickening of the plasmodium wall of the developing meronts (Fig. 6A–C). There were three variants (unikaryotic, diplokaryotic and potentially multi-nucleate) in the meront to sporont developmental process (Fig. 9). Sporonts with an electron dense cytoplasm were observed at a later stage in which there are vesicular (Vs) and granular structures (Gs) (Fig. 6C, G and I). Late sporonts/early sporoblasts were distinguishable by their completely thickened spore wall and the appearance of a polar tube (Fig. 6J). Sporoblasts

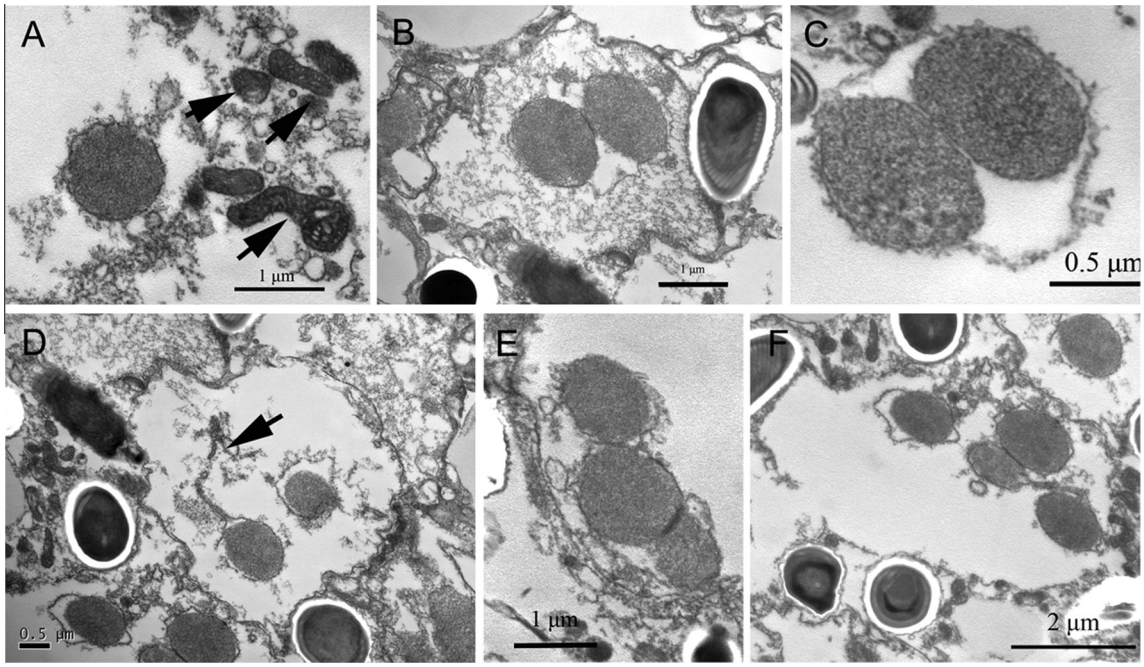

Fig. 5. Transmission electron micrographs of *V. necatrix* BM merogony and pre-sporogony in the adipose tissues of *B. mori*. In this phase, the nucleus was electron dense, and no endoplasmic reticulum was observed. (A) Ovoid meront; the arrows indicate host mitochondria. Scale bar, 1 μm. (B) Diplokaryotic meront. Scale bar, 1 μm. (C) Diplokaryotic meront undergoing binary fission. Scale bar, 0.5 μm. (D) Two separate meronts; the arrow shows a tube connected with meront. Scale bar, 0.5 μm. (E) The meront developmental stage with three connected nuclei observed in a sporophorous vesicle. Scale bar, 1 μm. (F) The meront development stage. There are two monokaryotic meronts and a diplokaryotic meront observed in a sporophorous vesicle. Scale bar, 2 μm.

possessed thick spore walls and a disorganized polar-tube structure (Fig. 6K). Late sporoblasts/mature spores had a completed structure and polar tubes arranged in coils (Fig. 7).

The mature spore shares a similar structure with other microsporidian species in that there are two large nuclei that occupy the central part of the cell. *V. necatrix* BM spores are longer than *N. bombycis* spores, with the polar tube arranged in a special structure, located in close proximity to the spore wall to the spore wall (Fig. 7A). The number of coils of the polar tube ranged from 13 to 17 according to the size of spores (Fig. 7B). The polar tube was fixed to the spore wall by the anchoring disc, a structure that has been observed in *V. necatrix* and some other *Vairimorpha* species. The granulated polaroplasts serve as an apparatus to fix the polar tube in the head of the spore and are visible in mature spores (Fig. 7C and D).

3.4. Phylogenetic relationship

Phylogenetic analysis of the small subunit rRNA showed that the pathogen described in this study formed one cluster with ssrRNA from two *V. necatrix* isolates and *Vairimorpha* sp. NIS-M12 (Fig. 8). In addition, the *V. necatrix* BM did not form one cluster with *N. bombycis* (82.30% homology). Our results also revealed that it showed 99.52% identity to *V. necatrix* 2007, 98.96% identity with *V. necatrix* 1999 and 98.16% identity with *Vairimorpha* sp. NIS-M12. The small subunit rRNA from *Vairimorpha cheracis* shared the lowest identity (80.85%) with that of *V. necatrix* BM. Analysis showed that the genetic distances between *V. necatrix* BM and two different isolates of *V. necatrix* were 0.001 and 0.004, respectively and are the two lowest among all values (Table 3).

Furthermore, the above result was also supported by another phylogenetic analysis based on their actin genes (Fig. 9). Indeed, the actin gene from *V. necatrix* BM showed 98.58%, 80.39% and 78.66% sequence identity with homologs from *V. necatrix*, *Nosema ceranae* and *N. bombycis*, respectively. In addition, two conserved genes, *HSP70* gene and *RPB1* from *V. necatrix* BM and *V. necatrix* also shared an extremely high level sequence identity (98.47% and 99.57%, respectively) (Figs. S2–S4). Together, our results demonstrated that these two isolates are homologous, but the presence of some slight differences between them indicates a divergence had occurred.

4. Discussion

There are more than ten known species of microsporidia belonging to five genera (*Nosema*; *Pleistophora*; *Vairimorpha*; *Thelohania*; *Endoreticulatus*) that can infect silkworms (Canning, 1953; Bhat et al., 2009). However, most of these microsporidia belong to the genera *Nosema* and *Vairimorpha* (Becnel et al., 1999; Hatakeyama et al., 1997; Kawakami et al., 1994). Studies on microsporidia within the silkworm host have paid more attention to *N. bombycis* than to *Vairimorpha* and other genera. This study is mainly focused on the pathology and ultrastructure of a new microsporidian isolate (*V. necatrix* BM) to determine whether the *V. necatrix* BM can transmit itself vertically to progeny silkworm and to understand the divergence between *V. necatrix* BM and other *Vairimorpha* species. As our results have shown, the silkworm symptoms of a *V. necatrix* BM infection were similar to those of an infection with *N. bombycis*.

Light microscopy and transmission electron microscopy studies indicated that *V. necatrix* BM was polymorphic throughout its life cycle. Merogony includes two pathways in the meront–sporont transitional stage that give rise to either monokaryotic or diplokaryotic sporonts. This characteristic is shared with other species from the family *Vairimorpha* (Wang et al., 2009) and other genera (Issi et al., 2012). The development of *V. necatrix* BM is significantly different in the midgut and fat body, possibly due to inconsistent infection of these tissues with microsporidia. Octospores, which

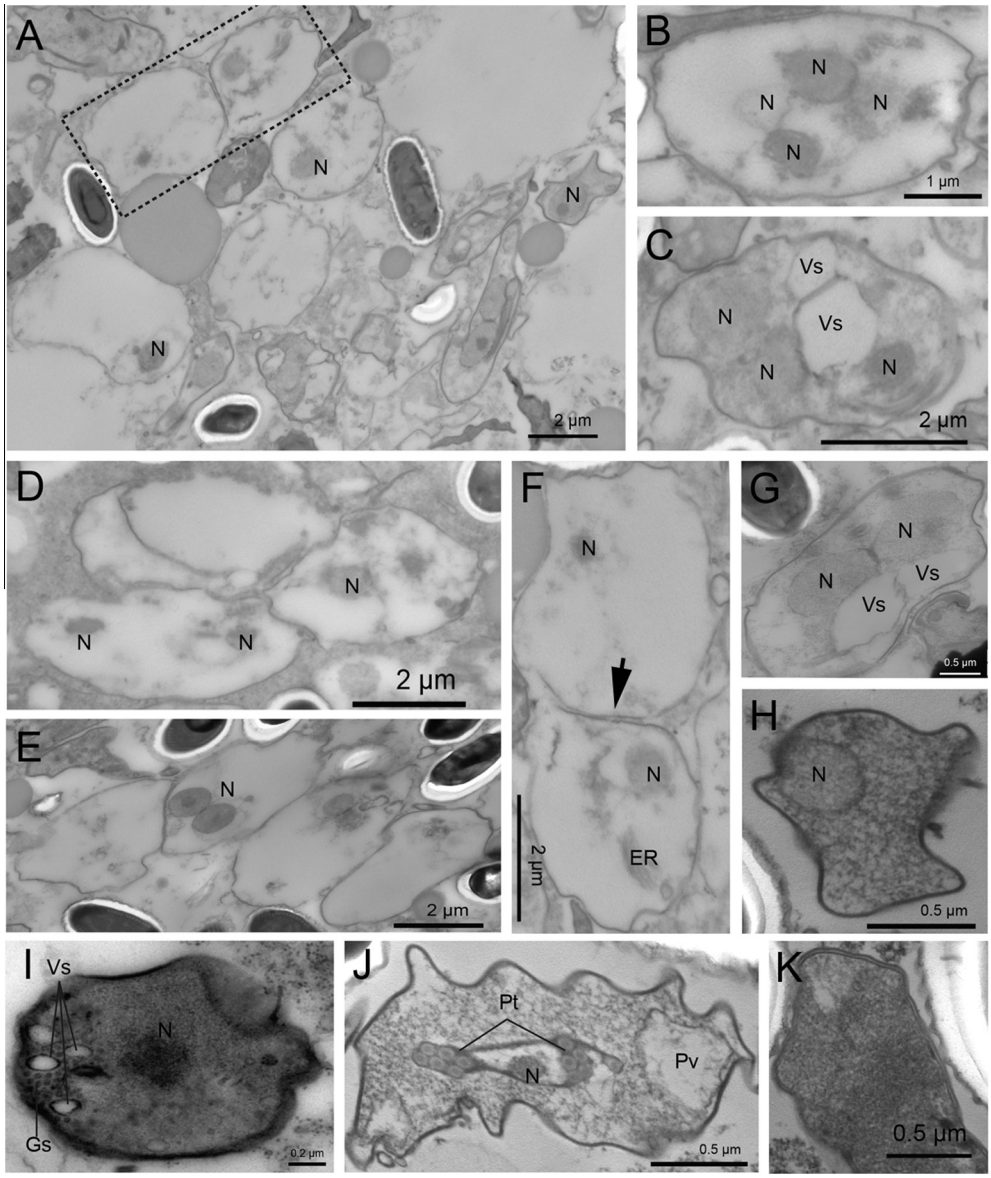

Fig. 6. Transmission electron micrographs of sporogony of *V. necatrix* BM in the midgut tissues of *B. mori*. The early sporogony phase involves thickening of the plasmodium wall of the developing meronts (A–C). *N* represents a single nucleus. There are three variants (unikaryotic, diplokaryotic and potentially multi-nucleate) in the meront to sporont developmental process. (A) Different shapes of sporonts in the midgut tissues, some with one or two nuclei were visible, in the others, the nucleus was not visible. (B; C) Sporonts with more than two nuclei were observed. (D; E) Early sporogony of apparent bi-nucleate spores. (F) The enlarged graph of the dotted box in figure A shows early sporont undergoing binary fission to produce two monokaryotic sporonts, the endoplasmic reticulum (*ER*) was visible. The arrow indicates new plasma membranes were in formation. (G) Diplokaryotic sporont, a double nuclear envelope was observed. (H) Monokaryotic sporont with electron dense cytoplasm. Sporonts with an electron dense cytoplasm are observed at a later stage in which there are vesicular (*Vs*) and granular structures (*Gs*) (C; G; I). (J) A late sporont/early sporoblast is discernible by its completely thickened plasma membranes and six coils of polar tubes (*Pt*) occupying the central part of the cell and posterior vacuole (*Pv*) positioned in posterior. (K) Sporoblasts possess thick spore walls and an in-organizing polar-tube structure. Scale bars in A; C; D; E; F are all 2 μm. Scale bars in G; H; J; K are all 0.5 μm. Scale bar in B is 1 μm. Scale bar in I is 0.2 μm.

were only observed in the moths, may reveal that spore karyotype status is influenced by environmental conditions, a phenomenon that has been reported in *V. necatrix* (Kramer, 1965).

Pathological and morphological studies of *V. necatrix* BM and *N. bombycis* reveal that there are many differences between them. Although there have been reports that the genera *Nosema* and *Vairimorpha* could not be separated into different clades using molecular characteristics (Tsai et al., 2003; Ku et al., 2007), the evidence from this study and previous studies have shown that *V. necatrix* BM is different from *N. bombycis* in terms of pathogenic characterization and life cycle due to its more complex and non-specific parasitic life cycle. The ultrastructure of this species is similar to some *Vairimorpha* species, but is different from other species from the *Vairimorpha* family in its subtle ultrastructural characteristics, including *Vairimorpha* sp M12 from Japan, *V. necatrix* isolated in the USA (Kramer, 1965), *V. plodiae* isolated in India (Kellen et al., 1968) and other species recently isolated from lepidopterous insects. The greatest divergence is in the merogony and sporogony stages. In the mature spore stages, there were differences in the number of polar tubes and the structure of the anchoring disc. These differences could be used as markers to distinguish different strains of *Vairimorpha* and to solve taxonomic conundrums.

Molecular phylogenetic analysis of this isolate revealed that it was closely related to the members of the *Vairimorpha* group (Liu et al., 2012). In result of such, we consider this isolate as a member of the *Vairimorpha* genus. A phylogenetic tree with more

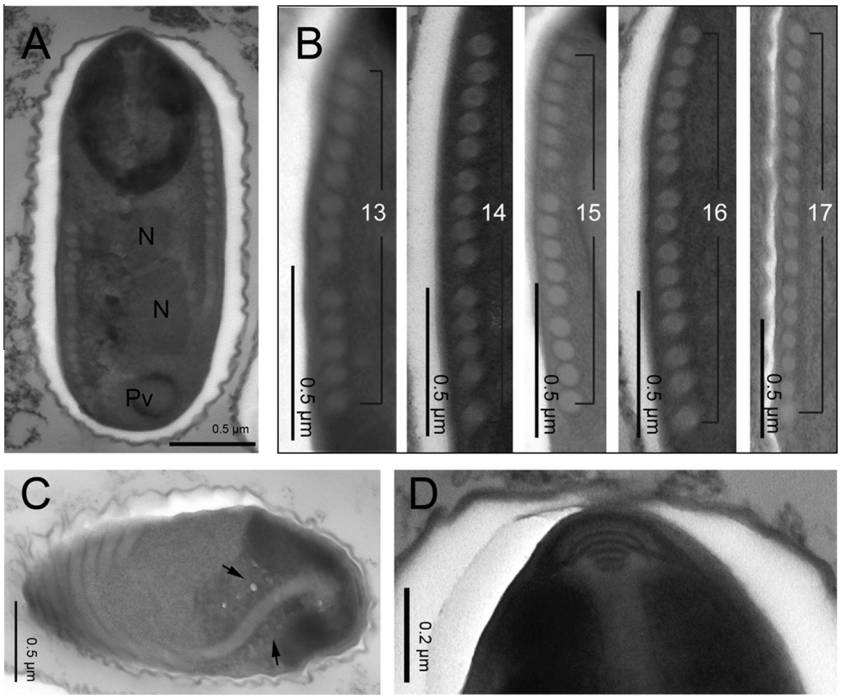

Fig. 7. Ultrastructure of mature spores in the fat body of *B. mori*. (A)The mature spore shares a similar structure with other microsporidian species in which there are two large nuclei that occupy the central part of the cell, and in the cross section polar tube is arranged in lines and cling to the spore wall. *N* represents nucleus; *Pv* represents posterior vacuole. Scale bar, 0.5 μm. The coils of polar tube are changed from 13 to 17 according to the size of spores (B). Scale bar, 0.5 μm. The granulated polaroplasts (arrows) serve as apparatuses to fix the polar tube in the head of the spore (C). Scale bar, 0.5 μm. The polar tube is fixed to the spore wall by the anchoring disc (D). Scale bar, 0.2 μm.

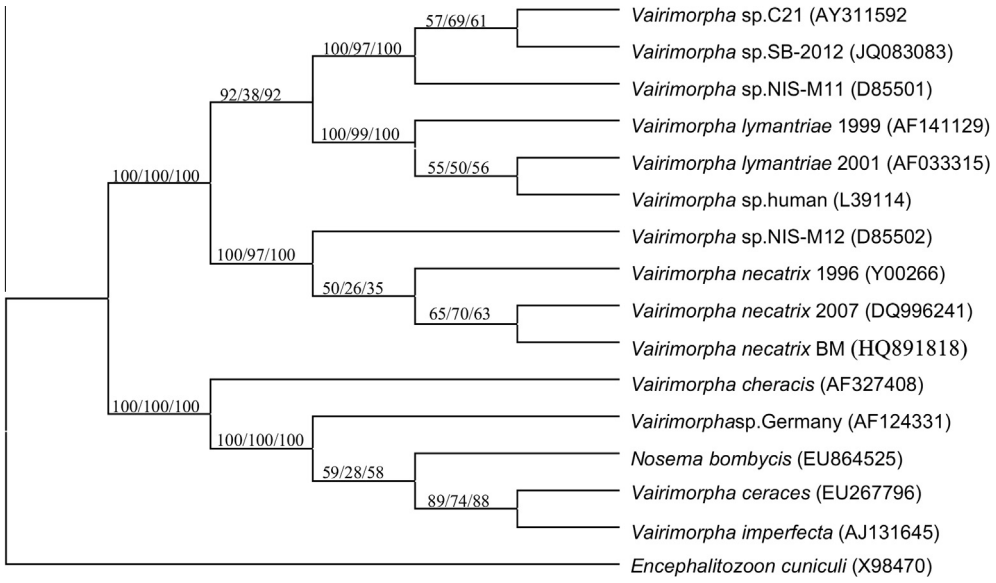

Fig. 8. Phylogenetic analysis of small subunit rRNA gene showing the relationship of *V. necatrix* BM with other microsporidia of the same genus and *N. bombycis*. *E. cuniculi* was included as the outgroup species. Phylogenetic tree was constructed by the neighbor-joining method, maximum parsimony method and minimum evolution method, respectively.

Vairimorpha species was constructed based on the SSU rRNA showing that this isolate was more closely related to *V. necatrix* than other *Vairimorpha* species. Three genes, conserved between species showed high homology between this isolate and *V. necatrix*. According to these morphological and molecular characteristics, we conclude that this strain was evolved from *V. necatrix* via species divergence which occurred a long time after the host changed.

Taxonomic Summary (*V. necatrix* BM).
V. necatrix (strain) *B. mori*.
Type host: *B. mori* (Lepidoptera: Bombycidae).
Other hosts: unknown.
Type locality: *B. mori* collected in Shan dong, China.
Site of infection: Numerous tissues including the midgut, Malpighian tubules, fat body, silk glands, muscles and testis. No infection in ovary.

Table 3
Analysis of the genetic distances between *Vairimorpha* species and other microsporidia.

	[1]	[2]	[3]	[4]	[5]	[6]	[7]	[8]	[9]	[10]	[11]	[12]	[13]	[14]	[15]
[1] *Vairimorpha necatrix* BM															
[2] *Vairimorpha ceraces*	0.188														
[3] *Vairimorpha* sp. Germany	0.183	0.007													
[4] *Vairimorpha imperfecta*	0.184	0.003	0.004												
[5] *Nosema bombycis*	0.183	0.005	0.006	0.002											
[6] *Vairimorpha cheracis*	0.178	0.029	0.028	0.026	0.028										
[7] *Vairimorpha* sp. *C21*	0.028	0.191	0.188	0.187	0.185	0.177									
[8] *Vairimorpha* sp. SB 2012	0.028	0.191	0.188	0.187	0.185	0.177	0.003								
[9] *Vairimorpha* sp. NIS-M11	0.026	0.191	0.188	0.187	0.185	0.177	0.003	0.002							
[10] *Vairimorpha lymantriae* 2001	0.03	0.192	0.189	0.188	0.187	0.181	0.021	0.021	0.019						
[11] *Vairimorpha lymantriae* 1999	0.03	0.19	0.188	0.187	0.185	0.18	0.02	0.02	0.018	0.001					
[12] *Vairimorpha sp.* human	0.029	0.193	0.19	0.189	0.188	0.182	0.02	0.02	0.018	0.001	0.002				
[13] *Vairimorpha necatrix* 2007	0.001	0.187	0.181	0.183	0.182	0.177	0.027	0.027	0.025	0.03	0.029	0.029			
[14] *Vairimorpha necatrix* 1996	0.004	0.188	0.183	0.184	0.183	0.178	0.028	0.028	0.026	0.031	0.03	0.03	0.003		
[15] *Vairimorpha sp.* NIS M12	0.007	0.191	0.186	0.187	0.186	0.181	0.03	0.03	0.029	0.033	0.033	0.033	0.006	0.007	
[16] *Encephalitozoon cuniculi*	0.423	0.458	0.457	0.456	0.456	0.448	0.427	0.424	0.425	0.426	0.426	0.424	0.423	0.423	0.424

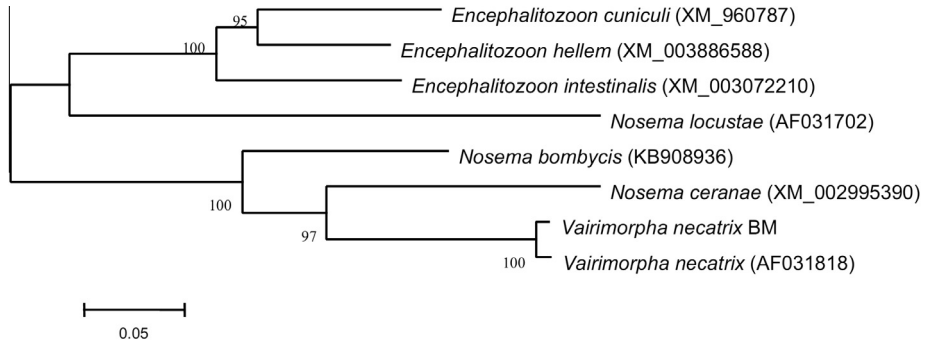

Fig. 9. Phylogenetic analysis of actin gene showing the relationship of *V. necatrix* BM with other microsporidia. Phylogenetic tree was constructed by the neighbor-joining method.

Transmission: Horizontal transmission (peros) and no vertical (transovarial) transmission (no spores observed in ovaries and developing oocytes). Evacuated spores in host tissues provide evidence of autoinfection.
Merogony: Binary fission.
Sporogony: Binary fission.
Spores: Oval, diplokaryotic, fresh spores measure $4.7 \pm 0.2 \times 2.1 \pm 0.2$ μm) with a granulated polaroplast and relatively small posterior vacuole. The polar filament is arranged in 13–17 coils in single layers.

Acknowledgments

We are grateful to Mr. Michael Galarnyk, Mr. Allen Pei in Nanoengineering department, UCSD and Dr. Scott Campbell from University of Exeter for manuscript language editing. We thank all the authors for their free-charged software cited and used in this article. This work is supported by the Grants from National Basic Research Program of China (No. 2012CB114604), Natural Science Foundation of China (No. 31272504, No. 30930067, No. 31001036, No. 31072089), National High-tech R&D Program (863 Program, No. 2012AA101301-3, No. 2013AA102507), Chongqing Science & Technology Commission (No. CSTC2010AA1003), the Program of Introducing Talents of Discipline to Universities (No. B07045).

Appendix A. Supplementary data

Supplementary data associated with this article can be found, in the online version, at http://dx.doi.org/10.1016/j.exppara.2014.05.001.

References

Becnel, J.J., Andreadis, T.G., 1999. Microsporidia in insects. In: Wittner, M., Weiss, L.M. (Eds.), The Microsporidia and Microsporidiosis. ASM Press, Washington, DC, pp. 447–501.
Bhat, S.A., Bashir, I., Kamili, A.S., 2009. Microsporidiosis of silkworm, *Bombyx mori* L. (Lepidoptera-Bombycidae): a review. Afr. J. Agric. Res. 4, 1519–1523.
Canning, E.U., 1953. A new microsporidian, *Nosema locustae n. sp.*, from the fat body of the African migratory locust, *Locusta migratoria* migratorioides R. & F. Parasitology 43 (3–4), 287–290.
Down, R.E., Bell, H.A., Kirkbride, S.A.E., Edwards, J.P., 2004. The pathogenicity of *Vairimorpha necatrix* (Microspora: Microsporidia) against the tomato moth, *Lacanobia oleracea* (Lepidoptera: Noctuidae) and its potential use for the control of Lepidopteran glasshouse pests. Pest. Manage. Sci. 60 (8), 755–764.
Goldsmith, M., Shimada, T., Abe, H., 2005. The genetics and genomics of the silkworm *Bombyx mori*. Annu. Rev. Entomol. 50, 71.
Hatakeyama, Y., Hayasaka, S., 2003. A new method of pebrine inspection of silkworm egg using multiprimer PCR. J. Invertebr. Pathol. 82 (3), 148–151.
Hatakeyama, Y., Kawakami, Y., Iwano, H., Inoue, T., Ishihara, R., 1997. Analyses and taxonomic inferences of small subunit ribosomal RNA sequences of five microsporidia pathogenic to the silkworm, *Bombyx mori*. J. Seric. Sci. Jpn., 66.
Huang, W.F., Tsai, S.J., Lo, C.F., Soichi, Y., Wang, C.-H., 2004. The novel organization and complete sequence of the ribosomal RNA gene of *Nosema bombycis*. Fungal Genet. Biol. 41 (5), 473–481.
Ishihara, R., 1969. The life cycle of *Nosema bombycis* as revealed in tissue culture cells of *Bombyx mori*. J. Invertebr. Pathol. 14 (3), 316–320.
Ishihara, R., Sohi, S.S., 1966. Infection of ovarian tissue culture of *Bombyx mori* by *Nosema bombycis* spores. J. Invertebr. Pathol. 8 (4), 538–540.
Issi, I.V., Tokarev, Y.S., Seliverstova, E.V., Voronin, V.N., 2012. Taxonomy of *Neoperezia chironomi* and *Neoperezia semenovaiae* comb. nov. (Microsporidia, Aquasporidia): lessons from ultrastructure and ribosomal DNA sequence data. Eur. J. Protistol. 48 (1), 17–29.
Kawakami, Y. et al., 1994. Comparison of chromosomal DNA from four microsporidia pathogenic to the silkworm *Bombyx mori*. Appl. Entomol. Zool. 29, 120.
Kellen, W., Lindegren, J., 1968. Biology of *Nosema plodiae* sp. n., a microsporidian pathogen of the Indian-meal moth, *Plodia interpunctella* (Hübner), (Lepidoptera: Phycitidae). J. Invertebr. Pathol. 11 (1), 104.
Kramer, J.P., 1965. *Nosema necatrix* sp. *n.* and *Thelohania diazoma* sp. *n.*, microsporidians from the armyworm *Pseudaletia unipuncta* (Haworth). J. Invertebr. Pathol. 7 (2), 117–121.

Ku, C.T., Wang, C.Y., Tsai, Y.C., Tzeng, C.C., Wang, C.H., 2007. Phylogenetic analysis of two putative *Nosema* isolates from Cruciferous Lepidopteran pests in Taiwan. J. Invertebr. Pathol. 95 (1), 71–76.

Li, R. et al., 2010. De novo assembly of human genomes with massively parallel short read sequencing. Genome Res. 20 (2), 265–272.

Liu, H., Pan, G., Li, T., Huang, W., Luo, B., Zhou, Z., 2012. Ultrastructure, chromosomal karyotype, and molecular phylogeny of a new isolate of microsporidian *Vairimorpha* sp BM (Microsporidia, Nosematidae) from *Bombyx mori* in China. Parasitol. Res. 110 (1), 205–210.

Liu, H. et al., 2008. Multiple rDNA units distributed on all chromosomes of *Nosema bombycis*. J. Invertebr. Pathol. 99 (2), 235–238.

Mitchell, M.J., Cali, A., 1993. Ultrastructural study of the development of *Vairimorpha necatrix* (Kramer, 1965) (Protozoa, Microsporida) in larvae of the corn earworm, *Heliothis zea* (Boddie) (Lepidoptera, Noctuidae) with emphasis on sporogony. J. Eukaryot. Microbiol. 40 (6), 701–710.

Nageswara, R.S., Muthulakshmi, M., Kanginakudru, S., Nagaraju, J., 2004. Phylogenetic relationships of three new microsporidian isolates from the silkworm *Bombyx mori*. J. Invertebr. Pathol. 86 (3), 87.

Pilley, B.M., 1976. A new genus, Vairimorpha (Protozoa: Microsporida), for *Nosema necatrix* Kramer 1965: pathogenicity and life cycle in *Spodoptera exempta* (Lepidoptera: Noctuidae). J. Invertebr. Pathol. 28 (2), 177–183.

Prasad, M. et al., 2005. SilkSatDb: a microsatellite database of the silkworm *Bombyx mori*. Nucleic Acids Res. 33 (suppl 1), D403–D406.

Saitou, N., Imanishi, T., 1989. Relative efficiencies of the fitch-margoliash, maximum-parsimony, maximum-likelihood, minimum-evolution, and neighbor-joining methods of phylogenetic tree construction in obtaining the correct tree. Mol. Biol. Evol. 6 (5), 514–525.

Saitou, N., Nei, M., 1987. The neighbor-joining method: a new method for reconstructing phylogenetic trees. Mol. Biol. Evol. 4 (4), 406–425.

Sato, R., Kobayashi, M., Watanabe, H., 1982. Internal ultrastructure of spores of microsporidans isolated from the Silkworm *Bombyx mori*. J. Invertebr. Pathol. 40 (2), 260–265.

Tamura, K., Dudley, J., Nei, M., Kumar, S., 2007. MEGA4: molecular evolutionary genetics analysis (MEGA) software version 4.0. Mol. Biol. Evol. 24 (8), 1596–1599.

Tsai, S.J., Lo, C.F., Soichi, Y., Wang, C.H., 2003. The characterization of microsporidian isolates (Nosematidae: Nosema) from five important Lepidopteran pests in Taiwan. J. Invertebr. Pathol. 83 (1), 51–59.

Wang, C.Y., Solter, L.F., Huang, W.F., Tsai, Y.C., Lo, C.F., Wang, C.H., 2009. A new microsporidian species, *Vairimorpha ocinarae n.* sp., isolated from *Ocinara lida Moore* (Lepidoptera: Bombycidae) in Taiwan. J. Invertebr. Pathol. 100 (2), 68–78.

Wang, L., Chen, K., Zhang, Z., Yao, Q., Gao, G., Zhao, Y., 2006. Phylogenetic analysis of *Nosema antheraeae* (microsporidia) isolated from Chinese oak silkworm, *Antheraea pernyi*. J. Eukaryot. Microbiol. 53 (4), 310.

Xia, Q. et al., 2004. A draft sequence for the genome of the domesticated silkworm (*Bombyx mori*). Science 306 (5703), 1937–1940.